

# Thermodynamic Properties of Spin Ladders with Cyclic Exchange

Alexander Bühler,<sup>\*</sup> Ute Löw,<sup>†</sup> Kai P. Schmidt,<sup>‡</sup> and Götz S. Uhrig<sup>§</sup>

*Institut für Theoretische Physik, Universität zu Köln, Zùlpicher Straße 77, 50937 Köln, Germany*

(Dated: November 2, 2018)

By high temperature series expansion and exact complete diagonalization the magnetic susceptibility  $\chi(T)$  and the specific heat  $C(T)$  of a two-leg  $S = 1/2$  ladder with cyclic (4-spin) exchange are computed. Both methods yield convincing results for not too small temperatures. We find that a small amount of cyclic exchange influences the thermodynamical properties significantly. Our results can serve as reliable basis for an efficient analysis of experimental data

PACS numbers: 05.10.-a, 75.40.Cx, 75.10.Jm, 75.50.Ee

## I. INTRODUCTION

Recently, it has been pointed out that both for spin ladder systems and the parent compounds of high- $T_c$  superconductors [1] in addition to the bilinear exchange also biquadratic ring exchange terms are important [2, 3, 4, 5, 6, 7]. In Refs. [8, 9, 10, 11, 12, 13, 14, 15, 16] the modification of the low temperature behavior due to this new exchange interaction has been discussed in detail. However, only little investigations [17] of the impact of this new type of interaction on the finite temperature properties are available up to now. Therefore, in this paper we address the question how the thermodynamic properties of two leg spin-1/2 ladders are modified by cyclic exchange interactions. In particular, the present work provides the appropriate high temperature series (HTSE) data and results from exact complete diagonalization (ED) [18] of the magnetic susceptibility and the specific heat. We expect that such an analysis constitutes an important supplement to the study of spin-ladders, furnishing additional information about couplings and interactions.

The model under study is given by the Hamiltonian

$$H = \sum_i \left( J_{\perp} \mathbf{S}_{1,i} \mathbf{S}_{2,i} + J_{\parallel} [\mathbf{S}_{1,i} \mathbf{S}_{1,i+1} + \mathbf{S}_{2,i} \mathbf{S}_{2,i+1}] \right. \\ \left. + 2J_{\text{cyc}} [(\mathbf{S}_{1,i} \mathbf{S}_{1,i+1})(\mathbf{S}_{2,i} \mathbf{S}_{2,i+1}) \right. \\ \left. + (\mathbf{S}_{1,i} \mathbf{S}_{2,i})(\mathbf{S}_{1,i+1} \mathbf{S}_{2,i+1}) - (\mathbf{S}_{1,i} \mathbf{S}_{2,i+1})(\mathbf{S}_{2,i} \mathbf{S}_{1,i+1})] \right) \quad (1)$$

where  $J_{\perp} > 0$  and  $J_{\parallel} > 0$  are the rung and leg couplings, respectively; the subscript  $i$  denotes the rungs and 1,2 the two legs.  $J_{\text{cyc}} > 0$  parametrizes the cyclic (4-spin) exchange.

In Sec. II we briefly sketch the methods we use. In Sec. III, results for the magnetic susceptibility  $\chi(T)$

$$\chi(\beta; J_{\parallel}, J_{\text{cyc}}) = \frac{\beta}{N} \frac{\text{tr} M^2 e^{-\beta H}}{\text{tr} e^{-\beta H}} = \frac{\beta}{N} \langle M^2 \rangle \quad (2)$$

and the specific heat  $C(T)$

$$C(\beta; J_{\parallel}, J_{\text{cyc}}) = \frac{1}{N} \frac{\partial}{\partial T} \left( \frac{-\frac{\partial}{\partial \beta} \text{tr} e^{-\beta H}}{\text{tr} e^{-\beta H}} \right) \quad (3)$$

are presented for the Hamiltonian in Eq. 1. We also discuss representations of our results which can be used to pinpoint the parameter regime from experimental data quickly.

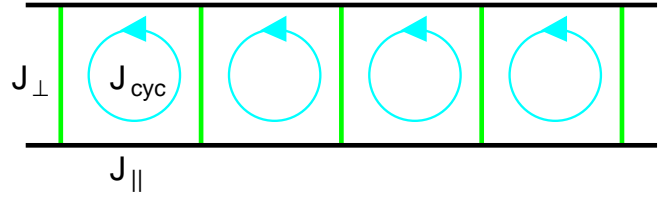


FIG. 1: Two-leg ladder with cyclic (4-spin) exchange

## II. METHODS

We use ED and the analytic method of HTSE. The computer aided calculations for the HTSE yield polynomials in the coupling parameters with fractions of integers as coefficients so that no accuracy is lost.

Details of our calculations can be found in Ref. [19] and details of the extrapolation schemes in Refs. [20, 21]. Further, the data are provided in electronic form so that it can be put to use quickly.

For both quantities  $\chi(T)$  and  $C(T)$  the results are provided up to order ten in the dimensionless inverse temperature  $\beta = J_{\perp}/T$ . The first orders for  $\chi(T)$  and  $C(T)$  are listed in Eqs. 14a and 14b, where  $x_{\text{cyc}} = J_{\text{cyc}}/J_{\perp}$  and  $x = J_{\parallel}/J_{\perp}$ . Higher orders are available electronically.

The bare truncated series are not sufficient to describe the quantities under study at low values of  $T$ . Padé representations [22] are used to enhance decisively the region of validity of the HTSE results. Additionally, we include low temperature information to enhance the region of validity even further. In some cases we can describe the susceptibility in the complete temperature regime. This

<sup>\*</sup>Electronic address: ab@thp.uni-koeln.de

<sup>†</sup>Electronic address: ul@thp.uni-koeln.de

<sup>‡</sup>Electronic address: ks@thp.uni-koeln.de

<sup>§</sup>URL: <http://www.thp.uni-koeln.de/~gu>; Electronic address: gu@thp.uni-koeln.de

is in particular true if the system is substantially gapped because the relevant correlation length remains finite restricted by the inverse of  $\max(k_B T/\hbar v, \Delta/\hbar v)$ , where  $v$  is a typical velocity of the excitations.

For a gapped system both  $C(T)$  and  $\chi(T)$  vanish for  $T \rightarrow 0$ . At finite but small temperatures the deviation from zero is exponentially small due to the spin gap. Furthermore, the leading power in  $T$  depends only on the dimensionality of the system [23]. The low temperature susceptibility for the ladder system can be expressed by

$$\chi(T) \approx T^{-\frac{1}{2}} e^{-\frac{\Delta}{T}} \quad \text{for } T \ll \Delta. \quad (4a)$$

An analogous expression is obtained for  $C(T)$

$$C(T) \approx T^{-\frac{3}{2}} e^{-\frac{\Delta}{T}} \quad \text{for } T \ll \Delta. \quad (4b)$$

Eqs. 4 provide additional information to bias the extrapolations. The value for the spin gap is obtained from Ref. [24].

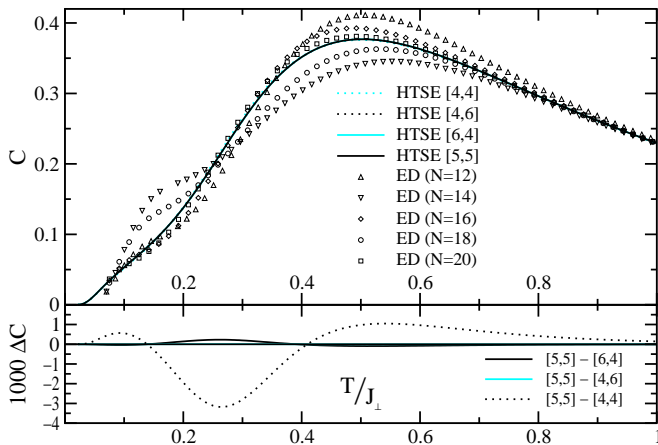


FIG. 2: Specific heat for  $x = 1$  and  $x_{\text{cyc}} = 0.1$ , upper plot:  $C(T)$  for various orders of Padé representations and ED results from  $N = 12$  to  $N = 20$ . lower plot: Differences between HTSE representations. The difference  $[5,5] - [4,6]$  cannot be discerned in the figure.

In contrast to our previous extrapolation schemes [20], here we employ and extend the method suggested in Ref. [21] to extrapolate the HTSE data for the specific heat. The main idea is to express the entropy  $S(T)$ , obtained from the HTSE data of the specific heat, in the new variable  $e - e_0$ , where  $e_0$  is the ground state energy and  $e = e(T)$  is the average energy per site. The temperature and the specific heat are then derived from the entropy as functions of  $e$ . The ground state energy is obtained from Ref. [24]. To incorporate the low temperature information from Eq. 4b the sum rule

$$e - e_0 = \int_0^T C(T') dT' \approx T^{\frac{1}{2}} e^{-\frac{\Delta}{T}} \quad (5)$$

is considered in the limit  $T \ll \Delta$ . Inverting the above equation provides an expression  $T(e - e_0)$ . Only an approximate solution is possible. Taking the logarithm of Eq. 5 and iterating twice in  $T$  leads to

$$T(y) \approx -\frac{\Delta}{\ln(\sqrt{\Delta}y)} \quad \text{for } y \ll 1 \quad (6)$$

with  $y = e - e_0$ . Combining Eqs. 5 and 6 and the sum rule

$$S = \int_0^T \frac{C(T')}{T'} dT' \approx T^{-\frac{1}{2}} e^{-\frac{\Delta}{T}} \quad \text{for } T \ll \Delta \quad (7)$$

yields the low temperature behavior of the entropy

$$S(y) \approx -\frac{y}{\Delta} \ln(\sqrt{\Delta}y) \quad \text{for } y \ll 1. \quad (8)$$

The logarithmic singularity at  $e = e_0$  ( $y = 0$ ) can be avoided by extrapolating the function

$$G(y) = y \partial_y \frac{S(y)}{y}. \quad (9)$$

The value of the gap  $\Delta$  is incorporated by requiring

$$G(y = 0) = -1/\Delta. \quad (10)$$

The entropy is then given by

$$S(e) = (e - e_0) \left( \int_0^e \frac{\tilde{G}(e')}{e' - e_0} de' - \frac{\ln 2}{e_0} \right) \quad (11)$$

where  $\tilde{G}$  is the Padé approximant of  $G$ . Wherever possible diagonal Padé representations, i.e. the same order in numerator and denominator are used. Exceptions to this rule will be stated explicitly; they are necessary where spurious poles occur. Comparison to ED results show that diagonal representations yield the best results, see Fig. 2. The convergence shown in the lower plot is very convincing. The plot compares to ED data for system sizes up to  $N = 20$ . It is systematic to the ED calculations that for increasing system sizes the results alternately yield an upper ( $N = 12, 16, 20$ ) or a lower ( $N = 14, 18$ ) bound on the specific heat for not too low temperatures. Therefore, the result for  $N = \infty$  should be in between the results with  $N = 18$  and  $N = 20$ , which is convincingly fulfilled by the HTSE extrapolations. The shoulders in the low temperature regime at  $T/J_{\perp} \lesssim 0.2$  are numerical artifacts.

It has to be noted that the precise knowledge of the ground state energy  $e_0$  is of particular importance for the extrapolation of the HTSE data for the specific heat. Even a small uncertainty of half a percent in  $e_0$  leads to significant differences in the specific heat at and below its maximum. The high temperature part is unaffected thereof. The ground state energy  $e_0(x, x_{\text{cyc}})$  is calculated up to order 11 in  $x$  and  $x_{\text{cyc}}$  in a high order series expansion about the limit of isolated rungs. We

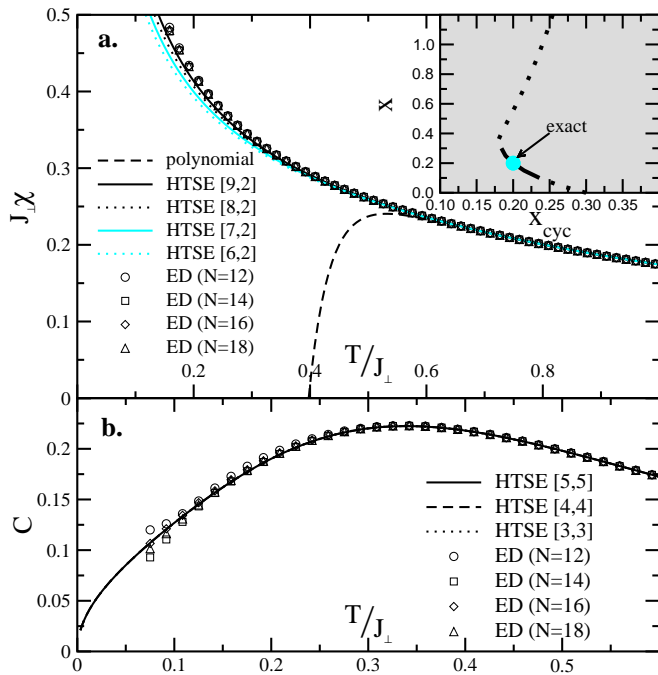


FIG. 3: Susceptibility (a.) and specific heat (b.) for  $x = 0.2$  and  $x_{\text{cyc}} = 0.2$  for various orders of Dlog-Padé representations and ED results for  $N = 12, 14, 16$ . HTSE representations in b. can not be resolved in the plot. Inset: Phase line with  $\Delta = 0$ , for details see Ref. [24].

set  $r = x_{\text{cyc}}/x = \text{const}$  and use standard Dlog-Padé approximants on  $de_0(x, rx)/dx$  which yield highly accurate results.

With the temperature as function of  $e$  at hand it is possible to represent also the susceptibility as function of  $e$ . The low temperature behavior from Eq. 4a can also be incorporated in the extrapolations. Unfortunately, the convergence of the extrapolations investigated is not as satisfying as for the specific heat. The low temperature regime is underestimated and the extrapolations are very sensitive to the order of numerator and denominator in the Padé representations. Most diagonal Padé approximants are not possible due to spurious poles. Hence we refrain from using a  $\chi(e)$  representation.

The extrapolation of the susceptibility follows Ref. [20]. Basically, the low temperature behavior from Eq. 4a is used to improve the representation. To incorporate the low temperature information it is advantageous to map the temperature regime to the interval  $[0, 1]$  via the substitution  $u = \beta/(1 + \beta)$ . All approximants are finite for  $u \rightarrow 1$  and the representations are no longer restricted

to diagonal Dlog-Padé approximants. All representations for  $\chi(T)$  are extrapolated with the same order of Dlog-Padé approximants to retain a consistent description of the HTSE results. We use the  $[n, 2]$ -Dlog-Padé representation in  $u$  with the only restriction  $n + 2 \leq 11$ . The representation chosen is checked in the limit of the (isotropic) ladder and the Heisenberg chain, where precise [25, 26, 27] or exact [28] results are available.

To assess the range of validity we investigate various orders of Dlog-Padé approximants. They are compared to the highest order available. The convergence is very satisfying. The orders 8 to 10 differ only by  $10^{-3}T/J_{\perp}$  from the 11th order for  $\chi$  (not shown). This observation does not change significantly for other sets of parameters considered.

Another important check is the comparison to ED results. In Fig. 3 data for the susceptibility and the specific heat are shown for the gapless point  $x = 0.2$  and  $x_{\text{cyc}} = 0.2$ , which is exactly known [24]. The inset shows the phase line where the gap vanishes. The results are obtained by a high order series expansion about the limit of isolated rungs. The solid line about the exact point shows the highly convergent results. The dotted lines give a sketch of the phase line for parameters far away from the exact point. The phase diagram is investigated in detail in Ref. [24]. Left to the phase line the system is in a gapped rung singlet phase. On increasing  $x_{\text{cyc}}$  the gap vanishes linearly in  $x_{\text{cyc}}$  and opens again linearly on the right of the phase line in a staggered dimer phase [29, 30].

To derive the low temperature behavior of  $C$  and  $\chi$  at the gapless point the exactly known triplet dispersion  $\omega(q) \propto q^2$  at  $q = \pi$  [24] is used. A similar analysis as in Ref. [23] yields

$$\chi(T) \approx \frac{1}{\sqrt{T}} \quad \text{for } T \ll 1 \quad (12a)$$

$$C(T) \approx \sqrt{T} \quad \text{for } T \ll 1. \quad (12b)$$

Using the sum rules mentioned above for the specific heat leads to an entropy

$$S(e) \approx (e - e_0)^{1/3} \quad \text{for } e - e_0 \text{ small.} \quad (13)$$

The entropy is extrapolated using a Dlog-Padé approximant biased to contain the extra information from Eq. 13.

The chosen representations of the HTSE results yield stable and trustworthy results for the calculated thermodynamical properties. Especially the experimentally interesting position and height of the maximum are sufficiently well described for quantitative predictions.

$$4T\chi = 1 + \left(-\frac{1}{4} - \frac{1}{2}x\right)\beta + \left(\left(\frac{1}{4} + \frac{3}{16}x_{\text{cyc}}\right)x - \frac{7}{32}x_{\text{cyc}}^2 - \frac{1}{16} + \frac{3}{16}x_{\text{cyc}}\right)\beta^2 + \mathcal{O}(\beta^3) \quad (14a)$$

$$16C = \left(\frac{3}{2} + 3x^2 + \frac{21}{8}x_{\text{cyc}}^2\right)\beta^2 + \left(\frac{3}{4} + \frac{3}{2}x^3 - \frac{27}{8}x_{\text{cyc}} - \frac{27}{8}x_{\text{cyc}}x^2 + \frac{45}{8}x_{\text{cyc}}^2 + \frac{45}{8}x_{\text{cyc}}^2x - \frac{9}{8}x_{\text{cyc}}^3\right)\beta^3 + \mathcal{O}(\beta^4) \quad (14b)$$

### III. RESULTS

Our aim is to provide results which show the quantitative behavior of the thermodynamic properties and in particular the effects of a cyclic spin exchange. With the help of computer algebra programs the HTSE results can be used easily to determine the model parameters of a substance under consideration. Only data of standard quantities like the magnetic susceptibility is necessary. The occurring ambiguity in determining the model parameters ([20] and see below) from only one quantity like  $\chi(T)$  can be resolved by the knowledge of other quantities, e.g. the spin gap  $\Delta$  or the magnetic specific heat  $C(T)$  as far as accessible experimentally.

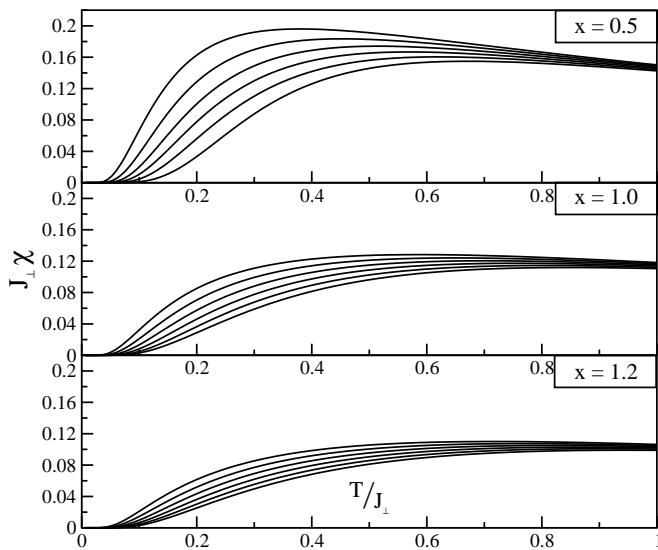


FIG. 4:  $\chi(T)$  for various values of  $x$  for  $x_{\text{cyc}} = 0, 0.02, 0.04, 0.06, 0.08$  and  $0.1$  in ascending order from right to left.

#### A. Susceptibility

Fig. 4 shows an overview of the magnetic susceptibility for various values of the cyclic exchange  $x_{\text{cyc}}$  and the leg coupling  $x$ . The choice of the shown parameter regime is taken from published values for substances presently investigated [10, 12, 16].

A general behavior for increasing  $J_{\text{cyc}}$  at fixed  $J_{\parallel}$  is the shift of an increasing  $\chi_{\text{max}}$  to lower temperatures. This effect is induced by the decrease of the whole dispersion, i.e. all energies are lowered [4, 24] and the global  $1/T$  factor which enhances the value of  $\chi_{\text{max}}$ . For increasing  $x$  this effect is weakened. The increasing leg coupling provides an additional antiferromagnetic coupling stabilizing the system against magnetic perturbations. Thus, an increasing  $x$  stabilizes the system and counteracts an increasing  $x_{\text{cyc}}$  which destabilizes it.

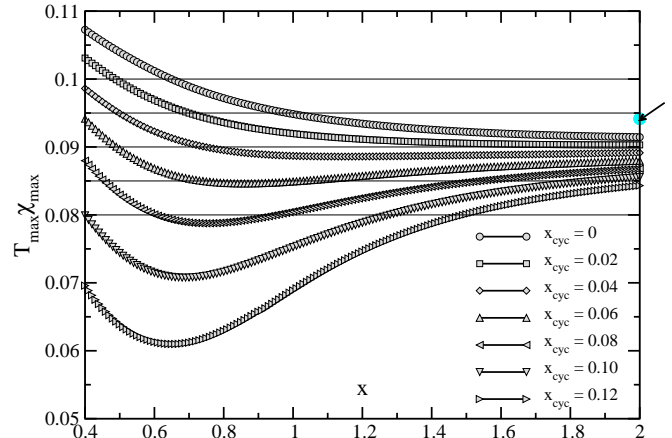


FIG. 5:  $\chi_{\text{max}}T_{\text{max}}$  versus  $x$  for  $x_{\text{cyc}} = 0, 0.02, 0.04, 0.06, 0.08$  and  $0.1$  in descending order. The symbols are the calculated data points from the HTSE. The filled circle on the right side indicates the  $\chi_{\text{max}}T_{\text{max}}$  value for an isotropic chain which is known exactly [28]. Horizontal lines show the constant values used to rescale  $\chi(T)$  in Fig. 6.

In Figs. 5 and 6 we address the information content of a measurement of  $\chi(T)$  (cf. [20]). Fig. 5 shows the energy-scale independent quantity  $\chi_{\text{max}}T_{\text{max}}$  which is a characteristic in experimental measurements. Note that for increasing  $x$  the differences between the curves for various values of  $x_{\text{cyc}}$  become smaller, because  $J_{\parallel}$  and  $J_{\perp}$  set the changing energy scale, whereas  $J_{\text{cyc}}$  stays constant. In the limit of large  $x$  the system approaches two independent chains with a decreasing relative interchain coupling induced by  $J_{\perp}$  and  $J_{\text{cyc}}$ .

Once the value of  $\chi_{\text{max}}T_{\text{max}}$  is measured the parameter set  $(x, x_{\text{cyc}})$  can be read off from Fig. 5. But there is still an ambiguity which cannot be resolved by a measurement of  $\chi(T)$  alone as illustrated in Fig. 6. There the

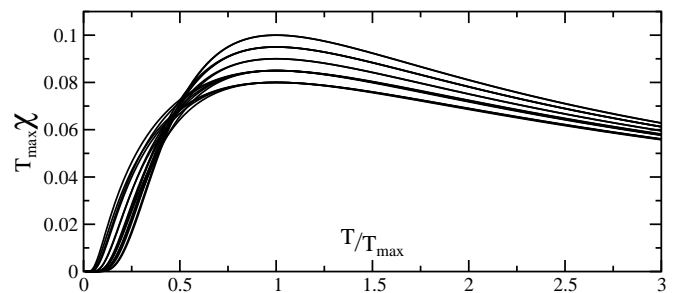


FIG. 6: Rescaled susceptibilities for  $\chi_{\text{max}}T_{\text{max}} = 0.1, 0.095, 0.09, 0.085, 0.08$  for the  $x$  and  $x_{\text{cyc}}$  values shown in Fig. 5

rescaled susceptibilities are depicted for the indicated values of  $\chi_{\text{max}}T_{\text{max}}$  in Fig. 5 (solid horizontal lines). The main feature in the susceptibility curves is the maximum.

For different sets of parameters for a specific value of  $\chi_{\max}T_{\max}$  the qualitative and quantitative behavior cannot be distinguished unless precise measurements in the low temperature regime are possible.

To summarize the latter investigations we state that with the present results of ED and HTSE it is difficult to ascertain all model parameters from the temperature dependence of the susceptibility alone, see also discussion in Ref. [20]. With the knowledge of detailed low temperature information this problem can be resolved.

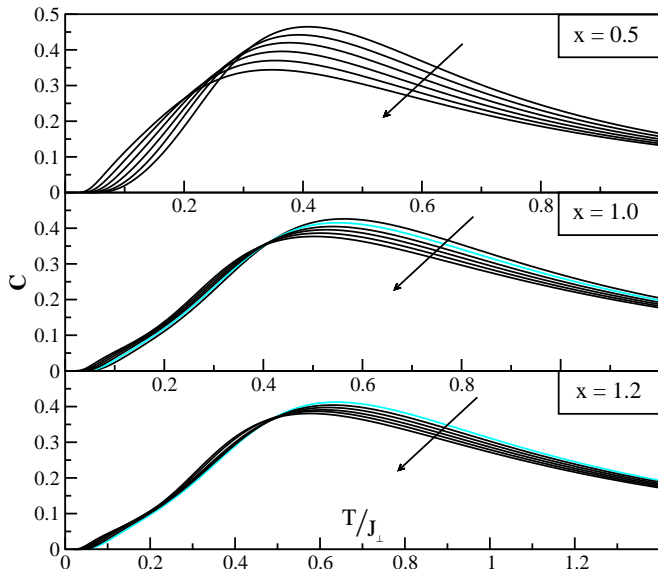


FIG. 7:  $C(T)$  for three values for  $x$  with  $x_{\text{cyc}} = 0, 0.02, 0.04, 0.06, 0.08$  and  $0.1$  in ascending order in direction of arrows. Gray lines show  $[6,4]$  Padé representations.

### B. Specific heat

Further information about the magnetic properties of substances can be obtained by measuring also the mag-

netic specific heat  $C(T)$ . We are aware, however, that it is difficult to extract the magnetic contribution from the measured specific heat if the energy scale of the lattice vibrations is of the same order as the magnetic couplings.

Once the magnetic specific heat is known the ambiguity in parameters can be resolved. Fig. 7 shows an overview of the magnetic specific heat for  $x = 0.5, 1, 1.2$  and  $x_{\text{cyc}} = 0, \dots, 0.1$ . For increasing leg coupling  $x$  and fixed  $x_{\text{cyc}}$  the position of  $C_{\max}$  shifts to higher temperatures and the height lowers slightly for  $x_{\text{cyc}} = 0, 0.02$ , it stays almost constant for  $x_{\text{cyc}} = 0.04, 0.06$ , and it increases slightly for  $x_{\text{cyc}} = 0.08, 0.1$ . For increasing cyclic exchange  $x_{\text{cyc}}$  and fixed leg coupling  $C_{\max}$  moves to lower temperatures and decreases. This behavior is induced by the decreasing overall dispersion, as discussed above.

### IV. CONCLUSIONS

We investigated the thermodynamic properties of the two-leg spin-1/2 ladder with cyclic exchange. We used two methods, ED and HTSE. The representation of the HTSE results were optimized by using Dlog-Padé and Padé approximants including the behavior of the considered quantities,  $\chi(T)$  and  $C(T)$  at low temperatures.

The results can serve as input for quick and easy data analysis to determine the model parameters. Especially the experimentally interesting position and height of the maxima of  $\chi(T)$  and  $C(T)$  are described quantitatively.

We showed that with the measurement of one quantity alone, e.g. the magnetic susceptibility it is difficult to determine all model parameters. Additional information like the spin gap or the specific heat helps fixing the parameters.

### Acknowledgments

The computations were done in the Regionales Rechenzentrum der Universität zu Köln with the kind support of P. Brühne. This work was supported by the DFG by Schwerpunkt 1073 and by SFB 608.

- 
- [1] E. Dagotto and T. M. Rice, *Science* **271**, 618 (1996).
  - [2] H. J. Schmidt and Y. Kuramoto, *Physica C* **167**, 263 (1990).
  - [3] Y. Honda, Y. Kuramoto, and T. Watanabe, *Phys. Rev. B* **47**, 11329 (1993).
  - [4] S. Brehmer, H.-J. Mikeska, M. Müller, N. Nagaosa, and S. Uchida, *Phys. Rev. B* **60**, 329 (1999).
  - [5] A. Reischl and E. Müller-Hartmann, *Eur. Phys. J. B* **28**, 173 (2002).
  - [6] T. Senthil and M. P. A. Fisher, *Phys. Rev. Lett.* **86**, 292 (2001).
  - [7] L. Balents, M. P. A. Fisher, and S. M. Girvin, *Phys. Rev. B* **65**, 224412 (2002).
  - [8] J. Lorenzana, J. Eroles, and S. Sorella, *Phys. Rev. Lett.* **83**, 5122 (1999).
  - [9] Y. Mizuno, T. Tohyama, and S. Maekawa, *J. Low Temp. Phys.* **117**, 389 (1999).
  - [10] M. Matsuda, K. Katsumata, R. S. Eccleston, S. Brehmer, and H.-J. Mikeska, *Phys. Rev. B* **62**, 8903 (2000).
  - [11] W. LiMing, G. Misguich, P. Sindzingre, and C. Lhuillier, *Phys. Rev. B* **62**, 6372 (2000).
  - [12] K. P. Schmidt, C. Knetter, and G. S. Uhrig, *Europhys. Lett.* **56**, 877 (2001).
  - [13] A. A. Katanin and A. P. Kampf, *Phys. Rev. B* **66**, 100403 (2002).
  - [14] R. Coldea, S. M. Hayden, G. Aeppli, T. G. Perring, C. D. Frost, T. E. Mason, S.-W. Cheong, and Z. Fisk, *Phys. Rev. Lett.* **86**, 5377 (2001).

- [15] M. Windt, M. Grüninger, T. Nunner, C. Knetter, K. Schmidt, G. S. Uhrig, T. Kopp, A. Freimuth, U. Ammerahl, B. Büchner, et al., *Phys. Rev. Lett.* **87**, 127002 (2001).
- [16] T. S. Nunner, P. Brune, T. Kopp, M. Windt, and M. Grüninger, *Phys. Rev. B, Rapid Comm.* (in press).
- [17] D. C. Johnston, M. Troyer, S. Miyahara, D. Lidsky, K. Ueda, M. Azuma, Z. Hiroi, M. Takano, M. Isobe, Y. Ueda, et al., *cond-mat/0001147* (2000).
- [18] K. Fabricius, A. Klümper, U. Löw, B. Büchner, T. Lorenz, G. Dhalenne, and A. Revcolevschi, *Phys. Rev. B* **57**, 1102 (1998).
- [19] A. Bühler, N. Elstner, and G. S. Uhrig, *Eur. Phys. J. B* **16**, 475 (2000).
- [20] A. Bühler, U. Löw, and G. S. Uhrig, *Phys. Rev. B* **64**, 024428 (2001).
- [21] B. Bernu and G. Misguich, *Phys. Rev. B* **63**, 134409 (2001).
- [22] A. Guttman, *Phase Transition and Critical Phenomena* (Academic Press, New York, 1989), vol. 13, chap. 1.
- [23] M. Troyer, H. Tsunetsugu, and D. Würtz, *Phys. Rev. B* **50**, 13515 (1994), There is a misprint in Eqs. (38) and (39),  $T/\Delta$  must be replaced by  $\Delta/T$ .
- [24] K. P. Schmidt, H. Monien, and G. S. Uhrig, to be published.
- [25] J. Oitmaa, R. R. P. Singh, and Z. Weihong, *Phys. Rev. B* **54**, 1009 (1996).
- [26] Z. Weihong, R. R. P. Singh, and J. Oitmaa, *Phys. Rev. B* **55**, 8052 (1997).
- [27] B. Frischmuth, B. Ammon, and M. Troyer, *Phys. Rev. B* **54**, R3714 (1996).
- [28] A. Klümper, *Z. Phys. B* **91**, 507 (1993).
- [29] M. Müller, T. Vekua, and H.-J. Mikeska, *cond-mat/0206081* (2002).
- [30] A. Läuchli, G. Schmid, and M. Troyer, *cond-mat/0206153* (2002).